

# Sleep need, the key regulator of sleep homeostasis, is indicated and controlled by phosphorylation of threonine 221 in salt-inducible kinase 3

Yang Li,<sup>1,2,3,4,†</sup> Chengang Li,<sup>2,3,4,†</sup> Yuxiang Liu,<sup>1,2,3,4,†</sup> Jianjun Yu,<sup>1,†</sup> Jingqun Yang,<sup>2,3,4</sup> Yunfeng Cui,<sup>5</sup> Tao V. Wang,<sup>1</sup> Chaoyi Li,<sup>2,3,4</sup> Lifan Jiang,<sup>2,3,4</sup> Meilin Song,<sup>2,3,4</sup> Yi Rao <sup>1,2,3,4,5,\*</sup>

<sup>1</sup>Laboratory of Neurochemical Biology, PKU-IDG/McGovern Institute for Brain Research, Peking-Tsinghua Center for Life Sciences, Peking-Tsinghua-NIBS (PTN) Graduate Program, School of Life Sciences, Department of Chemical Biology, College of Chemistry and Molecular Engineering, Peking University, Beijing 100871, China

<sup>2</sup>Institute of Physiology, Shenzhen Bay Laboratory, Shenzhen, Guangdong 518067, China

<sup>3</sup>Capital Medical University, Beijing 10069, China

<sup>4</sup>Chinese Institute for Brain Research, Changping Laboratory, Yard 28, Science Park Road, ZGC Life Science Park, Changping District, Beijing 102206, China

<sup>5</sup>Research Unit of Medical Neurobiology, Chinese Academy of Medical Sciences, Beijing 102206, China

\*Corresponding author: Laboratory of Neurochemical Biology, PKU-IDG/McGovern Institute for Brain Research, Peking-Tsinghua Center for Life Sciences, Peking-Tsinghua-NIBS (PTN) Graduate Program, School of Life Sciences, Department of Chemical Biology, College of Chemistry and Molecular Engineering, Peking University, 5 Yehyuan Road, Beijing 100871, China. Email: yrao@pku.edu.cn

<sup>†</sup>The first four authors are co-first authors.

## Abstract

Sleep need drives sleep and plays a key role in homeostatic regulation of sleep. So far sleep need can only be inferred by animal behaviors and indicated by electroencephalography (EEG). Here we report that phosphorylation of threonine (T) 221 of the salt-inducible kinase 3 (SIK3) increased the catalytic activity and stability of SIK3. T221 phosphorylation in the mouse brain indicates sleep need: more sleep resulting in less phosphorylation and less sleep more phosphorylation during daily sleep/wake cycle and after sleep deprivation (SD). Sleep need was reduced in SIK3 loss of function (LOF) mutants and by T221 mutation to alanine (T221A). Rebound after SD was also decreased in SIK3 LOF and T221A mutant mice. By contrast, SIK1 and SIK2 do not satisfy criteria to be both an indicator and a controller of sleep need. Our results reveal SIK3-T221 phosphorylation as a chemical modification which indicates and controls sleep need.

**Keywords:** sleep need, SIK3, T221, phosphorylation

## Introduction

Sleep is controlled by two processes: circadian (Process C) and homeostatic (Process S; [Borbély 1982](#); [Borbély et al. 2016](#)). Process C is the circadian biological clock which has been well studied at the molecular level since the discovery of the *Drosophila Period (Per)* gene in 1971 ([Konopka and Benzer 1971](#)) culminating in the understanding of a transcriptional-translational feedback loop conserved from insects to mammals including humans ([Allada et al. 1998](#); [Hardin et al. 1990](#); [King et al. 1997](#); [Renn et al. 1999](#); [Sehgal et al. 1994](#); [Toh et al. 2001](#)). By contrast, our understanding of Process S, the key component of homeostatic regulation of sleep, lags far behind that of Process C.

Process S is regulated by sleep need ([Borbély 1982](#); [Borbély et al. 2016](#); [Daan et al. 1984](#); [Tobler and Borbély 1986](#)), which can be measured by the spectral power in the  $\delta$  range (1–4 Hz) electroencephalogram (EEG) of non-rapid eye movement sleep (NREMS; [Dijk et al. 1987](#); [Franken et al. 2001](#); [Tobler and Borbély 1986](#); [Werth et al. 1996](#)).

Sleep need is regulated by prior wakeful experience ([Borbély 1982](#); [Suzuki et al. 2013](#)). During a natural day, there is gradual loss of sleep and concomitant increase of sleep need due to daily

activities (in the light phase for humans or the dark phase for mice), and a gradual decrease of sleep need due to sleep (in the dark phase for humans or the light phase for mice). Sleep need can also be increased by artificial sleep deprivation (SD): after the natural sleep is deprived (during the dark phase of humans or the light phase of mice), there is an increase of sleep need. Sleep is homeostatically regulated: loss of sleep in a natural day will be followed by sleep and artificial SD will result in a rebound of sleep.

A controller for sleep need should be necessary for EEG delta power in NREMS before and after SD, as well as sleep rebound after SD. So far, no molecule or chemical modification has been shown to be functionally required for all three (EEG  $\delta$  power before SD, EEG  $\delta$  power after SD and sleep rebound after SD).

An ideal indicator for sleep need should show correlation with sleep need in a natural sleep/wake cycle as well as that upon SD. So far, no molecule or chemical modification fulfill both criteria of a sleep need indicator.

In flies, we and others have found multiple genes whose loss of function (LOF) mutations significantly decreased sleep rebound after SD ([Cirelli 2009](#); [Crocker and Sehgal 2010](#); [Dai et al. 2019, 2021](#); [Deng et al. 2019](#); [Donlea et al. 2009, 2011](#); [Hendricks et al.](#)

2000; Liu et al. 2016; Qian et al. 2017; Shaw et al. 2000; Shi et al. 2021). However, there is no EEG delta power equivalent in flies to measure sleep need. No molecule or chemical modification could be established as an indicator of sleep need in flies.

In mice, the salt-inducible kinase 3 (SIK3) has been implicated in sleep regulation (Funato et al. 2016). It is based on the finding of a dominant gain of function (GOF) mutation *Sleepy*, which eliminated a segment containing serine 551 (S551), a target site for protein kinase A (PKA). Removal of S551 was known to increase SIK3 activity (Takemori et al. 2002). *Sleepy* increased sleep need (Funato et al. 2016). S551 mutation to alanine (A) (S551A) increased sleep need (Honda et al. 2018). However, both *Sleepy* and S551A are GOF mutations with increased SIK3 activities (Takemori et al. 2002). LOF SIK3 mutations have not been studied, and therefore physiological requirement of SIK3 in sleep need could not be established.

There are three SIKs in mammals (Feldman et al. 2000; Z. Wang et al. 1999; Xia et al. 2000). Mutations in SIK1 (S577A) and SIK2 (S587A) are equivalent to S551A in SIK3, and they also increased sleep need in mice (Park et al. 2020). Thus, all three SIKs were implicated in sleep need by GOF mutations, but none of the wild type (wt) mouse SIK genes has been shown to be physiologically necessary for sleep need, which requires evidence from LOF mutations. As we will show here, LOF SIK1 and SIK2 mutants were similar to the wt in sleep need, thus, neither SIK1 nor SIK2 is necessary for sleep need. It is essential to investigate LOF SIK3 mutants to determine whether SIK3 is necessary for sleep need.

While S551A of SIK3 increased sleep need (Honda et al. 2018), S551 phosphorylation did not change after SD (Funato et al. 2016; Honda et al. 2018). Thus, S551 phosphorylation does not indicate sleep need. Phosphorylation of its equivalent sites (S577 in SIK1 and S587 in SIK2) has not been previously studied in vivo, but it may not be productive to examine the phosphorylation of either SIK1 S577 or SIK2 S587 in light of our findings that neither SIK1 nor SIK2 is necessary for sleep need in mice.

Here we show T221 phosphorylation of SIK3 satisfies all criteria for a sleep need indicator and those for a sleep need controller.

## Materials and methods

### Antibodies

The primary antibodies used were anti-HDAC4 pS632 (1:1,000, 3424s, CST), anti-FLAG M2 HRP conjugated (1:2,000, A8592, Sigma), anti-SIK3 (1:500, Santa Cruz, sc-515408), anti-SIK3 pT221 (1:1,000, Abcam, ab271963), anti-PER2 (1:2,000, Abcam, ab227727), anti-PER2 pS662 (1:1,000, Abcam, ab206377), anti-Actin (1:4,000, Santa Cruz, sc-8342), anti-JNK (1:1,000, CST, 9252), anti-phospho-JNK (1:1,000, CST, 9251), anti-ERK1/2 (1:1,000, CST, 4695), anti-phospho-ERK (1:1,000, CST, 4370).

### Cell culture and transfection

HEK293T cells were obtained from ATCC and cultured in Dulbecco's modified Eagle's medium containing 10% fetal bovine serum (Gibco) and 1% Penicillin/Streptomycin (Gibco). HEK293T cells were transfected with Lipofectamine 3000 reagent (Thermo Fisher) according to the manufacturer's instructions and harvested 24–28 hrs after transfection.

### Immunoprecipitation and kinase assay in vitro

Plasmids expressing FLAG-tagged human SIK3 and mutants were transfected into HEK293T cells for immunoprecipitation. After 24 hrs, cells were collected and lysed with 1 ml lysis buffer [25 mM Tris-HCl pH 7.5, 150 mM NaCl, 5 mM MgCl<sub>2</sub>, 0.5% NP40,

0.25 M Sucrose, 1 mM DTT, 1 mM PMSF, 1 × protease inhibitor cocktail (Roche), 1 × phosphatase inhibitor II, 1 × phosphatase inhibitor III (Sigma)], before centrifugation of cell lysates at 20,000g for 30 min at 4 °C. Cell lysates were incubated with 10 μl anti-FLAG antibody-coated magnetic agarose beads, balanced by lysis buffer for 1 hr. Agarose beads were washed with 1 ml lysis buffer three times at 4 °C, before final washing with 100 μl 0.5 mg/ml 3xFLAG peptide buffer A at room temperature and storage at –80 °C. Kinase reactions were performed for 30 min at 37 °C by adding 10 μl kinase, 1 μg HDAC4 with a final concentration of 1 mM ATP. Samples were analyzed by immunoblotting with the indicated antibodies.

### Expression and purification of recombinant proteins

cDNAs for specific genes were cloned into pET-28a vector with indicated tags. Plasmids were transformed into *E. coli* BL21 cells and induced with 0.5 mM isopropyl-β-D-thiogalactoside (IPTG) at 18 °C for 16 hrs. Cells were harvested and suspended in Ni binding buffer (300 mM NaCl, 20 mM Tris-HCl, pH 7.5) supplemented with protease inhibitors. Cells were lysed by sonication and centrifuged at 14,000 rpm for 30 min. Supernatants were filtered by 0.45 μm filter and purified to 90% purity by tandem Ni<sup>2+</sup> and dextran affinity column. Pooled elution fractions were stained by Coomassie blue and stored at –80 °C.

### Animals

*Sik3* knockout *first(sik3-kof)* mice were purchased from CAM-SU GRC (Clone No. HEPD0744\_6\_E02). *Sik1* knockout (*Sik1ko*), *Sik2* knockout (*Sik2ko*) and *Sik3* point mutation mice were made as described later.

All experimental procedures were performed in accordance with the guidelines and were approved by the IACUC of Chinese Institute for Brain Research, Beijing. Mutant mice and wt littermates were maintained on a C57BL/6N background. Mice were housed under a 12 hr:12 hr light/dark cycle and controlled temperature and humidity conditions. Food and water were delivered ad libitum.

### Mouse protein preparation

Whole brains of mice were quickly dissected, rinsed with 1 × PBS and homogenized by homogenizer (Wiggins, D-500 Pro) in ice-cold lysis buffer (20 mM HEPES, 10 mM KCL, 1.5 mM MgCl<sub>2</sub>, 1 mM EDTA, 1 mM EGTA, 1 mM DTT, freshly supplemented with a protease and phosphatase inhibitor cocktail). Brain homogenates were centrifuged at 14,000 rpm for 15 min. Supernatants were carefully transferred to a new microtube. Protein concentrations of brain lysates were determined with the bicinchoninic acid (Thermo Fisher, 23225) assay and normalized to 2 mg/ml. Before immunoblotting, samples were kept in liquid nitrogen, if necessary.

### Quantitative real-time PCR

RNA was extracted from mouse brain lysates (a mixture of 3–4 mouse brains for each sample) using RNAPrep pure Tissue Kit (Tiangen, DP431). cDNA was synthesized using HiScript II 1st Strand cDNA Synthesis Kit (Vazyme, R211-01). Quantitative real-time PCR was performed using ChamQ SYBR qPCR Master Mix (Vazyme, R211-01) in the Roche LightCycler 96 Instrument. The following primers were used:

*Sik1*-Fw (5'-TCTGTCTGCAGGCTGAGAT-3'),  
*Sik1*-Rv (5'-ATAGCTGTGCCAGCAGACT-3'),

Sik2-Fw (5'-TGAGCAGGTTCTTCGACTGAT-3'),  
 Sik2-Rv (5'-AGATCGCATCAGTCTCACGTT-3'),  
 Sik3-Fw (5'-TTGTCAATGAGGAGGCACAC-3'),  
 Sik3-Rv (5'-TGTTAGGGGCCACTTGTAGG-3'),  
 Gapdh-Fw (5'-AGAACATCATCCCTGCATCC-3'),  
 Gapdh-Rv (5'-CACATTGGGGTAGGAACAC-3').

## Generation of point mutation and knock out mice

To select proper single-guide RNA (sgRNA), candidate sgRNAs were inserted into pCS-3G vector through Gibson assembly method, and the cleavage activity was verified by UCA method (Biocytogen). For each mutant mice, two sgRNAs were selected and transcribed in vitro to obtain RNAs (Sik1ko: 5'-gcggttgaggacgcacgggtgg-3' and 5'-gccagaagaccgcttgcgtgg-3'; Sik2ko: 5'-agtctgtctcgaatggaccagg-3' and 5'-tcagtgtagctccagatattgtgg-3'; Sik3ko: 5'-agtcattaacaacgactatgcgg-3' and 5'-gtcctcgcaaccagcgccgg-3' and Sik3<sup>221A/A</sup>: 5'-aggcgacatacctacctcctgg-3' and 5'-cgcggtggcactgatgccagg-3'). For Sik3<sup>221A/A</sup>, an additional donor vector was constructed with two ~1.5 kb homologous arms and donor sequence which covered exon 5 and 6 with nucleotide mutation from ACG to GCG (T221A) and additional sequence mutation to introduce AseI and BglII restriction enzyme sites for identification. sgRNAs only or sgRNAs and donor vector were injected into C57BL/6N mouse embryos. F0 mice were genotyped for the presence of recombination. F0 mice were mated with the counter C57BL/6N mice to obtain F1 offspring. The successful recombination was identified through Southern blot analysis in F1 mice. Mutant lines were back-crossed to C57BL/6N for at least five generations to exclude possible off-targeting.

## Electrode implantation surgery

EEG and EMG electrodes were made by sealing two EEG screws and two EMG wires in a 2 × 2 pin header with stainless steels (COONER WIRE AS633). The underside of pin header was covered by silicone rubber (Ausbond<sup>®</sup> 704) for insulation. Self-made electrodes were implanted into mice under anesthesia using isoflurane (3% for induction, 1.5% for maintenance) for EEG (AP-1 mm/ML-1.5 mm relative to bregma, AP-1 mm/ML-1.5 mm relative to posterior fontanel) and EMG (two wires inserted in the left and right neck muscles separately) acquisition. After implantation, the pin header was attached to the skull first by glue and then by dental cement. All mice were maintained individually for at least 5 days to recover from surgery. After recovery, mice were placed in the recording cage and tethered to an omni-directional arm (RWD Life Science Inc.) with a connection cable for 2 days of habituation before recording.

## Sleep recording and analysis

EEG and EMG data were recorded at a sampling frequency of 200 Hz with custom software (based on LabView 2020, National Instruments Corp.) for 2 consecutive days to analyze sleep/wake behavior under baseline conditions. The recording room was kept under a 12 hr:12 hr light/dark cycle and a controlled temperature (24–25°C). EEG/EMG data were initially processed by Accusleep (Barger et al. 2019), and then manually checked in SleepSign to improve accuracy and reduce analysis time. The data were classified in a 4 s epoch, the sleep stage was classified as a reference (Zhang et al. 2018). Briefly, wakefulness was scored as high amplitude and variable EMG and fast and low amplitude EEG; NREM was scored as high amplitude  $\delta$  (1–4 Hz) frequency EEG and low EMG tonus; REM was characterized as complete silence of EMG signals and low amplitude high-frequency  $\theta$  (6–9 Hz)-dominant EEG signal.

For power spectrum analysis, EEG was subjected to fast Fourier transform analysis with a hamming window method by SleepSign, yielding power spectra between 0 and 25 Hz with a 0.39 Hz bin resolution. State EEG power spectra represent the mean of power distribution for each state-corresponding epoch, i.e. NREMS, REMS, WAKE, during a diurnal recording period. The hourly NREMS  $\delta$ -power density indicates the average of  $\delta$ -power density as a percentage of  $\delta$ -band power (1–4 Hz) to total power (0–25 Hz) for each NREM epoch contained in an hour. Epochs containing movement artifacts were marked and excluded automatically in the spectra analysis by a custom algorithm, which initially summed up the power for each epoch at all frequency bins, calculating the difference of total power between each adjacent epochs and figuring out the abnormal value among these differences. The threshold T of differences was determined by visual inspection based on the distribution graph of these differences, epochs which contributed to those differences greater than T were identified and discarded. The state episode was defined as a continuous and single state epoch, NREM episode was defined as at least three continuous NREM epochs and was ended by REM epoch or at least three wakefulness epochs. REM or WAKE episode consists of at least three consecutive REM epochs or wakefulness epochs, respectively. The number and average duration of episode were defined as episode number and episode duration, respectively.

## Sleep deprivation

Sleep deprivation was manually carried out by preventing mice from sleep using a stick during ZT 0–6. This will ensure mice were awake during deprivation and reduce additional stress. Rebound of each stage was calculated as cumulative changes of WAKE/NREM/REM duration after SD compared to duration in the same ZT before SD. Changes of  $\delta$  power was calculated as  $\delta$  power post-SD minus  $\delta$  power pre-SD.

## Statistics

Statistical analysis was performed with GraphPad Prism 8.0.2 (GraphPad Software). Kruskal–Wallis test followed by Dunn's posttest was used to compare mean results from different lines. Two-way ANOVA followed by Turkey's multiple comparisons test was used to compare power spectrum between different lines. Statistical significance is denoted by asterisks: \*P < 0.05, \*\*P < 0.01, \*\*\*P < 0.001. Error bars in the graphs represent mean  $\pm$  SEM.

## Results

### Specific recognition of phosphorylated T221 in SIK3 by a monoclonal antibody in vitro and in vivo

SIKs from different species share a general structure with a catalytic domain, a ubiquitin-associated domain and a C terminal domain (Dai et al. 2021; Sakamoto et al. 2018; Wein et al. 2018). There are multiple sites of phosphorylation in a SIK protein, among which targets for PKA have been well studied: PKA usually negatively regulates SIK activities (Berggreen et al. 2012; Henriksson et al. 2012; MacKenzie et al. 2013; Patel et al. 2014; Sonntag et al. 2018; Takemori et al. 2002).

T221 of SIK3 is not a target site for PKA. It was found to change after SD by mass spectrometry (MS; Funato et al. 2016), but it has not been studied whether its level changes during a natural day of sleep/wake cycle. In order to examine natural changes more easily than relying on MS, we needed an antibody which could recognize phosphorylated T221. We tested the specificity of a rabbit monoclonal antibody (MAb) and found that it could recognize

the phosphorylated T221 of SIK3 in human embryonic kidney (HEK) cells transfected with a cDNA expressing SIK3 fused in-frame to the FLAG epitope tag (Fig. 1a). The MAb did not recognize T221 of SIK3 if the cell lysate was treated by a phosphatase (Fig. 1a). The MAb also did not recognize SIK3 if the amino acid residue at 221 was mutated to alanine (T221A) or to glutamic acid (T221E) in HEK cells (Fig. 1a). These results show that T221 phosphorylated in HEK cells is recognized by the anti-SIK3 phospho-T221 MAb.

To examine whether T221 phosphorylated in mice can be specifically recognized by the anti-SIK3 phospho-T221 MAb, we eliminated the SIK3 gene by gene targeting. We found that SIK3 knockout caused embryonic lethality, with a few mice born with the SIK3<sup>-/-</sup> genotype among hundreds of wt mice. While the number of SIK3<sup>-/-</sup> mice were too low to allow behavior or EEG analysis, we did manage to use them for protein analysis to confirm that the protein recognized by the MAb was absent in SIK3<sup>-/-</sup> mice while that in the wt was recognized by both the anti-SIK3 antibodies and the anti-SIK3 phospho-T221 MAb (Fig. 1b).

By the CRISPR-CAS9 method, we generated mice carrying the point mutation T221A (Fig. 5). SIK3 protein was detected in T221A mutant mice, whereas T221A was not recognized by the MAb (Fig. 1c), again demonstrating the specificity of the anti-phospho-T221 MAb in mice.

Taken together, our results provide *in vitro* and *in vivo* evidence that phospho-T221 in SIK3 can be recognized specifically by the anti-SIK3 phospho-T221 MAb.

### Significance of T221 for SIK3 catalytic activity

Histone deacetylase 4 (HDAC4) is a known substrate of SIK3 (Wang B *et al.* 2011). We used it to test the catalytic activities of SIK3 and its mutants. We transfected HEK cells with a cDNA construct expressing the FLAG-tagged SIK3 and found SIK3 immunoprecipitated with the anti-FLAG antibody to be active in phosphorylating HDAC4 (Fig. 1d “Control” lanes on the right), but this activity was reduced if SIK3 was treated with phosphatases (Fig. 1d “Phosphatase” lanes on the left).

T221A mutant of the full-length SIK3 expressed in HEK cells was not active in phosphorylating HDAC4 (Fig. 1e).

A shorter version of SIK3 containing amino acid residues 59–558 was also active in phosphorylating HDAC4 (Fig. 1f, WT), but T221A mutant of SIK3 59–558 was inactive (Fig. 1, a and f).

Surprisingly, the activity of SIK3-T221E immunoprecipitated from HEK was lower than the wt SIK3 in phosphorylating HDAC4 (Fig. 1e), though T221E was higher than T221A in phosphorylating HDAC4 (Fig. 1e). T221E mutation in SIK3 59–558 reduced but did not eliminate its activity (Fig. 1f).

Results from SIK3 catalytic activity show that SIK3-T221A could be used as a LOF mutant for SIK3, whereas SIK3-T221E could not be used as a simple GOF mutant for SIK3. We note that, rather than being more active mutants, S to D mutations in SIK3 (S551D), SIK1 (S587D) and SIK2 (S577D) were all less active than their corresponding wt (Honda *et al.* 2018; Park *et al.* 2020), with S to D mutants ending up with phenotypes qualitatively similar to those of S to A mutants (Honda *et al.* 2018; Park *et al.* 2020). In the case of these SIK phospho-site mutants, it was not helpful to use E or D mutants to find mutants more active than wt SIK proteins, making it meaningful to examine the *in vivo* phenotypes of only S or T to A mutants.

### Importance of T221 for SIK3 protein stability

We obtained *Sik3* knockout first (*Sik3-kof*) mutant mice through the insertion of bacterial *lacZ* trapping cassette to early terminate the

transcription of *Sik3* (Fig. 2a). *Sik3-kof/+* and *Sik3-kof/Sik3-kof* were both viable with a reduction of SIK3 mRNA expression (Fig. 2b) and SIK3 protein (Fig. 2, d and e). The anti-phospho-T221 MAb could recognize a band in *Sik3-kof/+* and *Sik3-kof/Sik3-kof* mice but the level of phospho-T221 also depended on the gene dosage (Fig. 2e). Therefore, *Sik3-kof* was used as a partial LOF mutant for SIK3.

With our T221A mutant mice, we found that the mRNA levels of SIK3 in +/221A and 221A/221A mice were similar and both were lower than that in the wt (Fig. 2c). It could also recognize a band in +/221A mice but not in 221A/221A mice (Fig. 2e). All these results further confirmed the specificity of the MAb *in vivo*.

Interestingly, while the mRNA levels of SIK3 were similar in +/221A and 221A/221A mice, the level of SIK3 protein was lower in 221A/221A mice than that in +/221A mice (Fig. 2, f and g). Phospho-T221 could be detected in +/221A mice but not in 221A/221A mice (Fig. 2f).

While the reduction of SIK3 mRNA level could partially explain the reduction of SIK3 protein in 221A/221A mice compared to the wt (+/+) (Figs. 1c and 2f), the finding that the level of SIK3 protein in 221A/221A mice was lower than that in +/221A mice could only be explained by reduced protein synthesis or stability caused by T to A mutation at residue 221 of SIK3.

Phosphorylation is well known to regulate protein stability. For example, in the case of the PER protein involved in circadian regulation of animals from *Drosophila* to humans, phosphorylation at multiple sites regulates its stability (Toh *et al.* 2001; Xu *et al.* 2005, 2007). To directly investigate SIK3 protein stability, we transfected cDNA constructs expressing either wt SIK3 or T221 SIK3 with a FLAG tag into HEK cells. After cycloheximide treatment to inhibit protein synthesis, levels of SIK3 were followed to examine SIK3 protein stability over the next 24 hrs (Fig. 2, h and i). There was a reduction of SIK3 protein in 2 hrs, but it was stable for the next 22 hrs (Fig. 2, h and i). By contrast, the level of SIK3-T221A protein decreased continuously over 24 hrs (Fig. 2, h and i).

Thus, both *in vivo* (Fig. 2f) and *in vitro* (Fig. 2, h and i) results are consistent with the idea that T221 phosphorylation enhances the stability of SIK3 protein.

### Indication of sleep need by T221 phosphorylation

Sleep need decreases with more sleep and increases with less sleep (Dijk *et al.* 1987; Franken *et al.* 2001; Suzuki *et al.* 2013; Tobler and Borbély 1986; Werth *et al.* 1996). To investigate whether T221 phosphorylation in SIK3 indicates sleep need, we first examined T221 phosphorylation in daily natural sleep/wake cycle. Mice were kept at a 12 hr dark/12 hr light schedule, with zeitgeber time (ZT) 0 as the beginning of the light phase when mice started to sleep and ZT12 as the beginning of the night when mice usually woke up.

We collected brains from 12 mice every 3 hrs over 36 hrs. While the level of actin did not change, T221 phosphorylation was highest at ZT0, decreasing to its lowest point at ZT12, returning gradually to peak again at ZT24 before decreasing again for another 12 hrs (Fig. 3, a and b).

The correlation of the level of T221 phosphorylation (Fig. 3, a and c) with the level of SIK3 protein further supports our conclusion from previous studies (Fig. 2, e and f) that T221 phosphorylation stabilizes SIK3 protein.

We collected brains from SIK3-T221A mutant mice every 6 hrs over 24 hrs, and found that the level of SIK3 protein did not change (Fig. 3, d and e). This result indicates that T221 phosphorylation stabilizes SIK3 protein *in vivo*.

We used the MAb recognizing phospho-T221 to confirm increased T221 phosphorylation after 6 hrs of SD (Fig. 3, f and h).

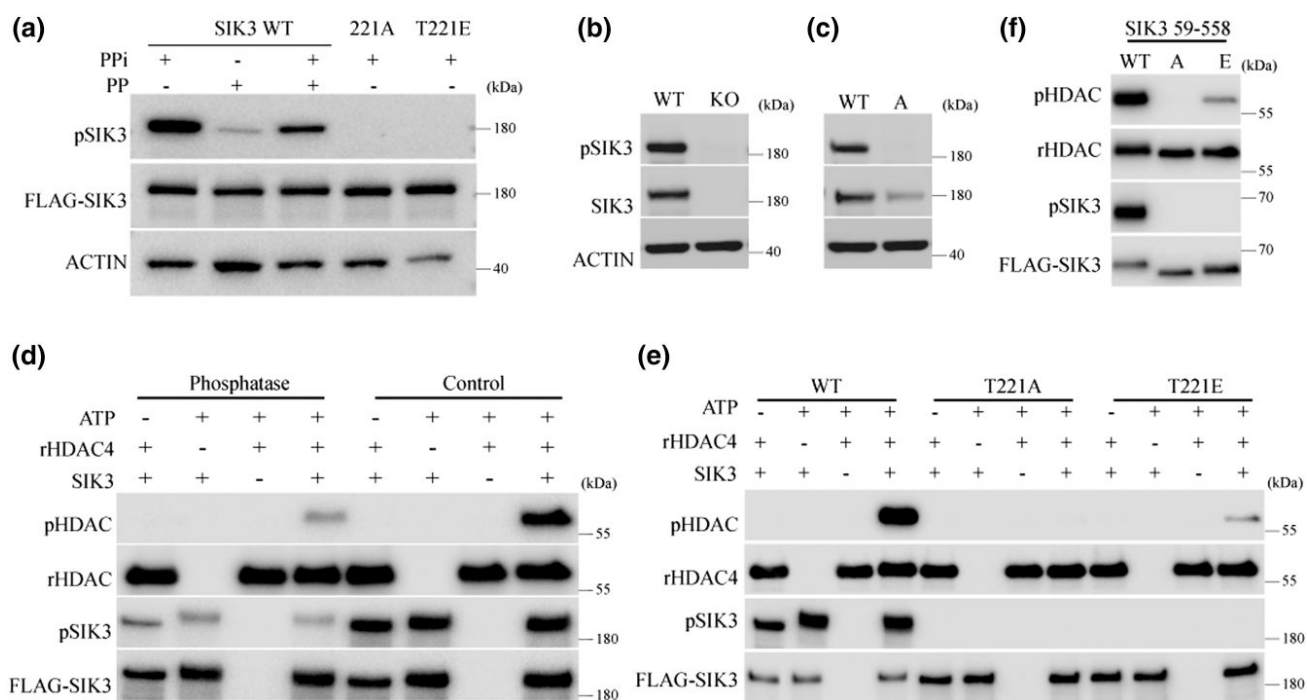


**Fig. 1.** T221 phosphorylation and SIK3 catalytic activity. a) Specificity of anti-SIK3 pT221 mAb in HEK293T cells. HEK293T cells were transfected with indicated plasmids and harvested 24 hrs after transfection. Extracts were subjected to Western blot analysis (WB) with indicated antibodies. ("p" indicates phosphophosphorylated amino acid residues). b) Immunoblotting with anti-SIK3 pT221 and anti-SIK3 antibodies of brain homogenates from *Sik3*<sup>+/+</sup> and *Sik3*<sup>-/-</sup> mice. c) Immunoblotting with anti-SIK3 pT221 and anti-SIK3 antibodies of brain homogenates from *Sik3*<sup>+/+</sup> and *Sik3*<sup>221A/A</sup> mice. d) SIK3 is regulated by phosphorylation at T221 site. FLAG-SIK3 was immunoprecipitated and pre-treated with or without  $\lambda$ -phosphatase for 1 hr at 37 °C. HDAC4 phosphorylation was detected by an antibody against phospho-HDAC4. e) The enzymatic activity of SIK3 WT protein is higher than those of T221E and T221A SIK mutant proteins. Indicated proteins were immunoprecipitated and assayed as in d. f) The enzymatic activity of SIK3 59–558 WT protein is higher than those of T221E and T221A SIK mutant proteins. Indicated proteins were immunoprecipitated and assayed as in d. HDAC4 with FLAG tag used in panel d, e, and f was expressed and purified from bacterial. The detection was through anti-FLAG antibody.

Consistent with our demonstration that T221 phosphorylation stabilizes SIK3 protein, the level of SIK3 protein also correlated with SIK3 phosphorylation with and without SD (Fig. 3, f and g). The levels of kinases such as ERK and JNK did not change with SD, nor the levels of ERK or JNK phosphorylation change with SD (Fig. 3f).

Our results reveal that the phosphorylation of SIK3 at T221 indicates sleep need.

### Lack of requirement for SIK1 and SIK2 in sleep need

SIK3 was first discovered for its role in sleep through *Sleepy* mutants, in which a segment in SIK3 including S551 was deleted, alleviating PKA-mediated negative regulation (Funato et al. 2016). S551 in SIK3 are equivalent to S577 in SIK1 and S587 in SIK2 (Park et al. 2020). Single-point mutations of SIK3 S551A, SIK1 S577A and SIK2 S587A all led to loss of PKA phosphorylation of these sites and increased their function (Honda et al. 2018; Park et al. 2020). All three point mutations increased sleep need in mice (Honda et al. 2018; Park et al. 2020). While these results suggest that all three SIK proteins regulate sleep need, the very nature of GOF made it not possible to establish a physiological requirement for any of the SIK proteins in regulating sleep need.

To investigate whether SIK1 or SIK2 is required for sleep need, we generated mice with their SIK1 or SIK2 gene deleted (Supplementary Figs. 1 and 2). Unlike SIK3 knockout mutation, which caused embryonic lethality, these knockout mice were viable and were subject to our experimental analysis of sleep

need. Our knockout strategies eliminated the expression of SIK1 (Supplementary Fig. 1f) and SIK2 mRNAs (Supplementary Fig. 2f).

$\delta$  power is a measure of EEG activity in the 1–4 Hz range, in slow-wave sleep (SWS, NREM sleep in humans), and reflects sleep need (Borbély 1982; Daan et al. 1984; Dijk et al. 1987; Franken et al. 2001; Tobler and Borbély 1986; Werth et al. 1996). No parameters for sleep or sleep need were changed in either kind of mutants (Supplementary Figs. 1 and 2). Sleep need as measured by  $\delta$  power EEG was not significantly different among *SIK1*<sup>+/+</sup>, *SIK1*<sup>+/-</sup>, or *SIK1*<sup>-/-</sup> mice (Supplementary Fig. 1d) at any time point over 24 hrs (Supplementary Fig. 1e). Similarly, sleep need as measured by  $\delta$  power EEG was not different among *SIK2*<sup>+/+</sup>, *SIK2*<sup>+/-</sup>, or *SIK2*<sup>-/-</sup> mice (Supplementary Fig. 2d) at any time point over 24 hrs (Supplementary Fig. 2e). These results show that neither SIK1 nor SIK2 is physiologically required for sleep need.

### Functional significance of SIK3 in sleep need

SIK3 elimination caused embryonic lethality and those that were born grew slowly, leaving us without sufficient number of SIK3 knockout mice for EEG analysis. Partial LOF *Sik3*-kof mutants (Fig. 2, a, b and d) allowed us to investigate physiological requirement of SIK3 in sleep need.

Daytime wake duration was significantly longer in *Sik3*-kof/*Sik3*-kof (-/-) mice when compared with +/+ mice (Fig. 4a). Daytime rapid eye movement (REM) sleep duration was significantly less in *Sik3*-kof/*Sik3*-kof (-/-) mice than that in +/+ mice (Fig. 4a). Sleep or wake episode durations and episode numbers were not significantly different between *Sik3*-kof/*Sik3*-kof (-/-) mice and wt mice (Supplementary Fig. 3a and b).

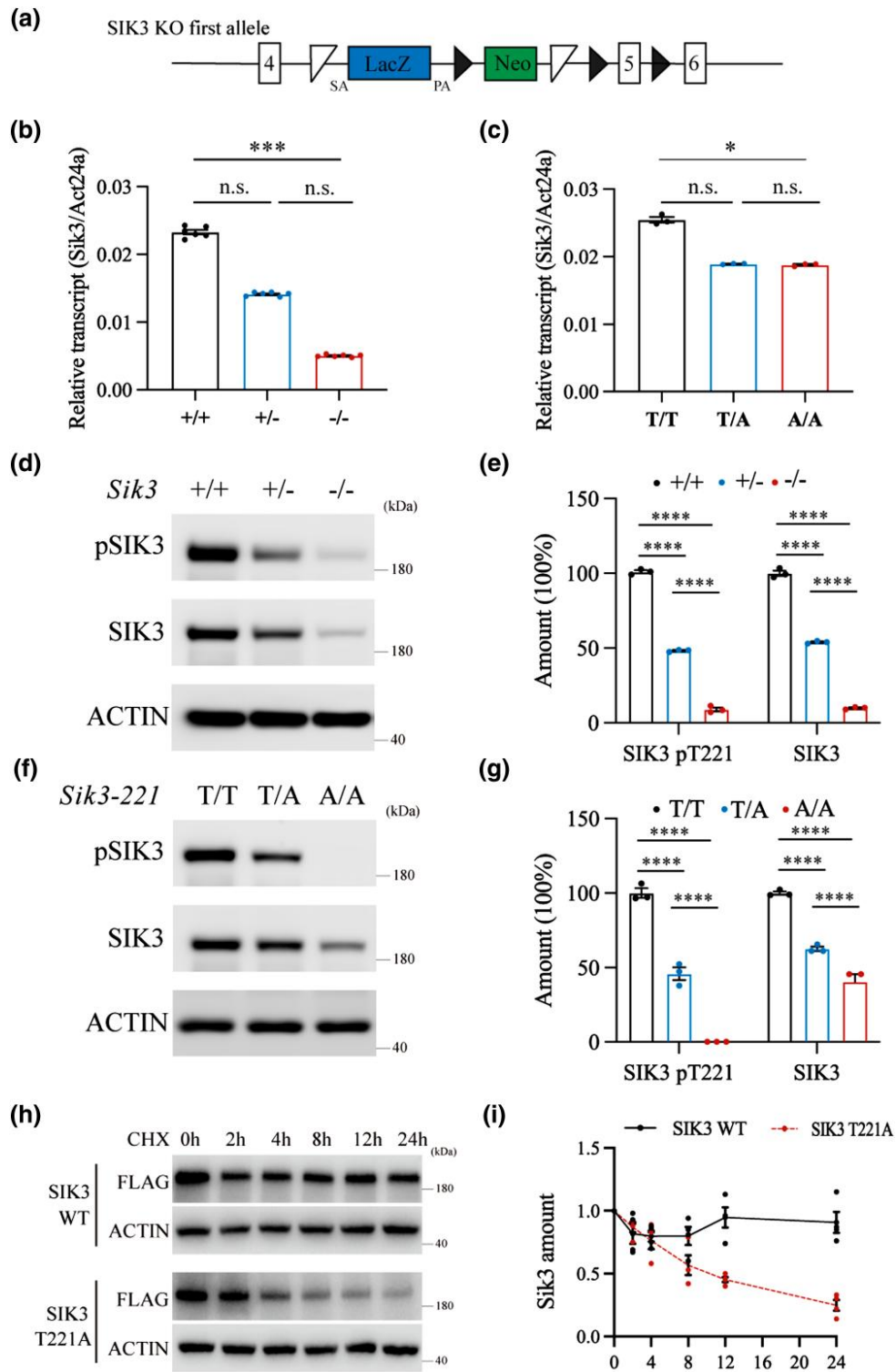


**Fig. 2.** T221 phosphorylation and SIK3 protein stability. a) A schematic diagram of the *Sik3*-kof allele. Insertion of lacZ-polyA into intron 4 led to *Sik3* transcription termination after exon 4. The white triangle represents FRT, and the black triangle represents Loxp. SA: splice acceptor, PA: poly A. b) Relative *Sik3* mRNA expression levels in the brains of *Sik3*<sup>+/+</sup> (n = 6), *Sik3*<sup>+/-</sup> (n = 6), and *Sik3*<sup>-/-</sup> (n = 6) mice. Kruskal-Wallis test with Dunn's posttest. \*\*\*P < 0.001. Error bars represent standard error of the mean (SEM). c) Relative *Sik3* mRNA expression levels in the brains of *Sik3*<sup>+/+</sup> (n = 3), *Sik3*<sup>+/-</sup> (n = 3), and *Sik3*<sup>221A/A</sup> (n = 3) mice. Kruskal-Wallis test with Dunn's posttest. \*P < 0.05. Error bars represent SEM. d) Levels of SIK3-T221 phosphorylation and SIK3 protein expression in the brains from *Sik3*<sup>+/+</sup> (n = 3), *Sik3*<sup>+/-</sup> (n = 3), and *Sik3*<sup>-/-</sup> (n = 3) mice. e) Quantification of SIK3-T221 phosphorylation and SIK3 protein level in panel d. Two-tailed unpaired t-test. \*\*\*\*P < 0.0001. Error bars represent SEM. f) Levels of SIK3-T221 phosphorylation and SIK3 protein expression in the brains of *Sik3*<sup>+/+</sup> (n = 3), *Sik3*<sup>+/-</sup> (n = 3), and *Sik3*<sup>221A/A</sup> (n = 3) mice. g) Quantification of SIK3-T221 phosphorylation and SIK3 protein level in panel f. Two-tailed unpaired t-test. \*\*\*\*P < 0.0001. Error bars represent SEM. h) SIK3 protein degradation analyzed in HEK293T cells. Cells were transfected with SIK3 WT or T221A plasmid and cultured for 24 hrs. Transfected cells were treated with 200 mM cycloheximide (CHX) before harvest at indicated time points. Equal amounts of extracts were subjected to immunoblot analysis with indicated antibodies. i) Quantification of SIK3 protein level in (h). Error bars represent SEM

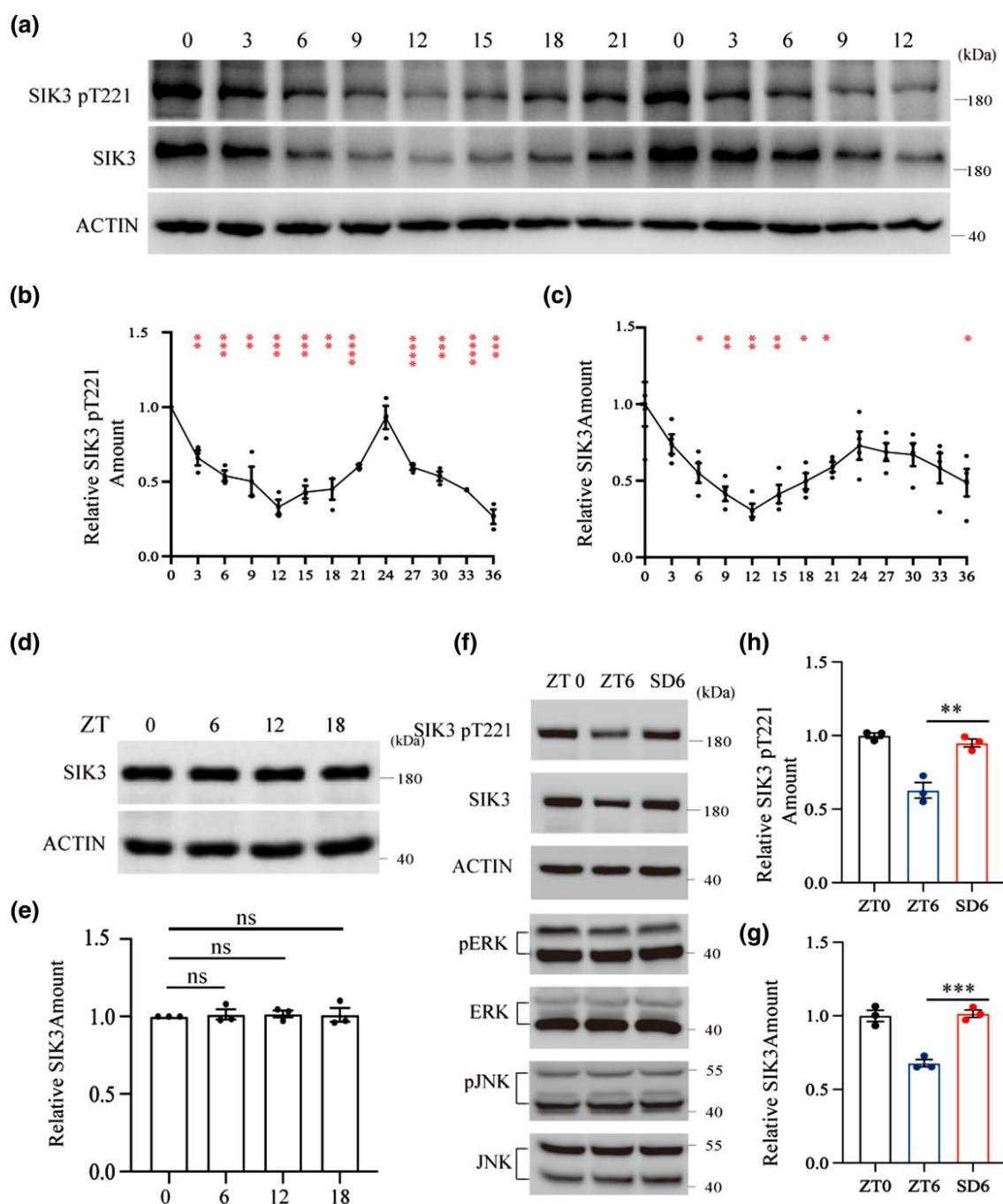


**Fig. 3.** Dynamics of SIK3 protein and T221 phosphorylation in a sleep/wake cycle and after sleep deprivation. a) Temporal profile of SIK3 protein level and T221 phosphorylation level in mouse brains ( $n = 12$  at each time point). ZT: zeitgeber time. b) The quantification of T221 phosphorylation level in panel a.  $**P < 0.01$ ,  $***P < 0.001$ ,  $****P < 0.0001$ . Error bars represent SEM. c) The quantification of SIK3 protein level in panel a.  $*P < 0.05$ ,  $**P < 0.01$ . Error bars represent SEM. d) SIK3 protein level in brains of SIK3-T221 mutant mice ( $n = 3$  at each time point). e) The quantification of SIK3 protein level in panel d. ns: no significance, Error bars represent SEM. f) The effect of sleep deprivation on SIK3 and T221 phosphorylation in mouse brains ( $n = 3$  at each time point). g) The quantification of T221 phosphorylation level in panel f.  $***P < 0.001$ , Error bars represent SEM. h) The quantification of SIK3 protein level in panel f.  $***P < 0.001$ , Error bars represent SEM.

Analysis of the EEG in *Sik3-kof* mutants showed that, during the NREM stages, power spectrum in the delta range (1–4 Hz) was significantly decreased: those in *Sik3-kof/Sik3-kof* ( $-/-$ ) mice were significantly lower than those in  $+/+$  and  $+/-$  mice (Fig. 4b). Delta power density (the ratio of 1–4 Hz delta power to overall 1–25 Hz EEG power) during NREM over a 24 hrs plot was significantly reduced in *Sik3-kof* mutants (Fig. 4c), especially during the night phase when sleep need accumulated in mice, at multiple time points, NREM  $\delta$  density in *Sik3-kof/Sik3-kof* ( $-/-$ ) mice was significantly lower than those in  $+/+$  and  $+/-$  mice (Fig. 4c).

Sleep need decreased gradually during light phase, when mice usually fell asleep, and increased gradually during dark phase, when mice were often awake. In the wt,  $\delta$  power densities at ZT16, 17, 18, 19, 20 and 22 were all significantly higher than those at ZT9, 10 and 11 (Fig. 4d). In *Sik3-kof/+* ( $-/+$ ) mice,  $\delta$  power densities at ZT16, 17, 18, 19, 20, 21 and 22 were all significantly higher than those at ZT9, 10 and 11 (Fig. 4d). However, in *Sik3-kof/Sik3-kof* ( $-/-$ ) mice, only  $\delta$  power density at ZT20 was significantly higher than those at ZT9 and ZT10, with no significantly at any other time point (Fig. 4d). These results indicate that SIK3 was necessary for accumulation of

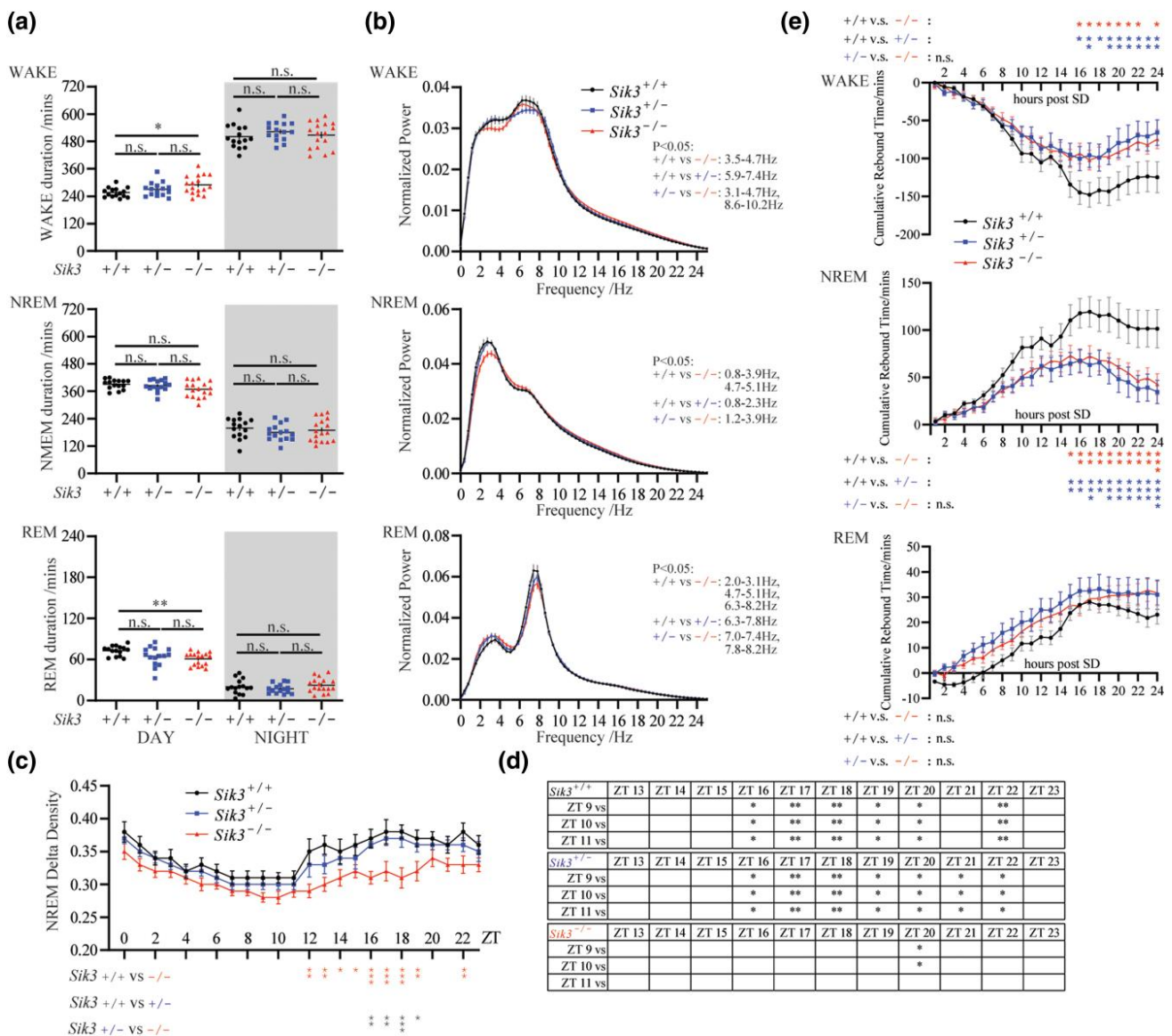


**Fig. 4.** SIK3 and sleep need in mice. a) The duration of WAKE, NREM and REM in *Sik3*<sup>+/+</sup> (n = 15), *Sik3*/*Sik3*-kof (<sup>+/-</sup>) (n = 15), and *Sik3*-kof/*Sik3*-kof (<sup>-/-</sup>) (n = 17) mice. \*P < 0.05, \*\*P < 0.01, Kruskal–Wallis test with Dunn’s posttest. Error bars represent SEM. b) EEG power spectrum of WAKE, NREM and REM states in *Sik3*<sup>+/+</sup> (n = 15), *Sik3*<sup>+/-</sup> (n = 15), and *Sik3*<sup>-/-</sup> (n = 17). Two-way ANOVA with Tukey’s posttest, P < 0.05 pairs were listed on the right. Error bars represent SEM. c, d) NREM  $\delta$ -power density of *Sik3*<sup>+/+</sup> (n = 15), *Sik3*<sup>+/-</sup> (n = 15), and *Sik3*<sup>-/-</sup> (n = 17). Two-way ANOVA with Tukey’s posttest, statistical comparison among genotypes listed below, and statistical comparison among different times listed on (d). \*P < 0.05, \*\*P < 0.01, and \*\*\*\*P < 0.0001. Error bars represent SEM. e) Accumulated WAKE loss, and NREM, REM sleep gain of *Sik3*<sup>+/+</sup> (n = 11), *Sik3*<sup>+/-</sup> (n = 12), and *Sik3*<sup>-/-</sup> (n = 11) after 6 hrs of SD. Two-way ANOVA with Tukey’s posttest, \*P < 0.05, \*\*\*\*P < 0.0001. Error bars represent SEM.

sleep over the active phase in mice. In short, accumulation of sleep need was dramatically reduced in the absence of SIK3.

To investigate involvement of SIK3 in homeostatic sleep regulation, we carried out 6 hrs of SD and analyzed changes of sleep homeostasis. In wt mice, NREM and REM rebounded after SD, with WAKE duration reduced (Fig. 4e). NREM rebound and WAKE reduction were significantly less in *Sik3*-kof mutant mice than those in wt mice (Fig. 4e). Curiously, REM rebound in *Sik3*-kof mutant mice was not different from that in wt mice.

Results *Sik3*-kof mutant mice show that SIK3 is required for sleep need and for NREM sleep rebound after SD.

### Functional significance of SIK3-T221 phosphorylation in sleep need

Our SIK3-T221A mutant mice allowed investigation of the physiological requirement of T221 phosphorylation in sleep need. T221A

mutants exhibited shorter NREM sleep duration (Fig. 5a), especially during the dark phase, with no change in REM sleep duration. Sleep or wake episode durations and episode numbers were not significantly different between T221A mutant mice and wt mice (Supplementary Fig. 4a and b). The specific decrease of NREM sleep duration in T221A mutant mice suggests possible reduction of homeostatic sleep pressure.

EEG spectrum analysis showed reduced  $\delta$  power density during NREM in T221A/T221A mutant mice as compared to wt mice (Fig. 5b). During the light phase, T221A mutants were similar to wt mice in decreasing sleep need, as the  $\delta$  power density decreased at a similar pace in T221A mutant and wt mice (Fig. 5c). During the dark phase the delta power of wt mice increased significantly whereas that in T221A mutants did not significantly change (Fig. 5c). The increase of  $\delta$  power density from ZT 9–11 (when mice had slept for a day) to ZT 18–23

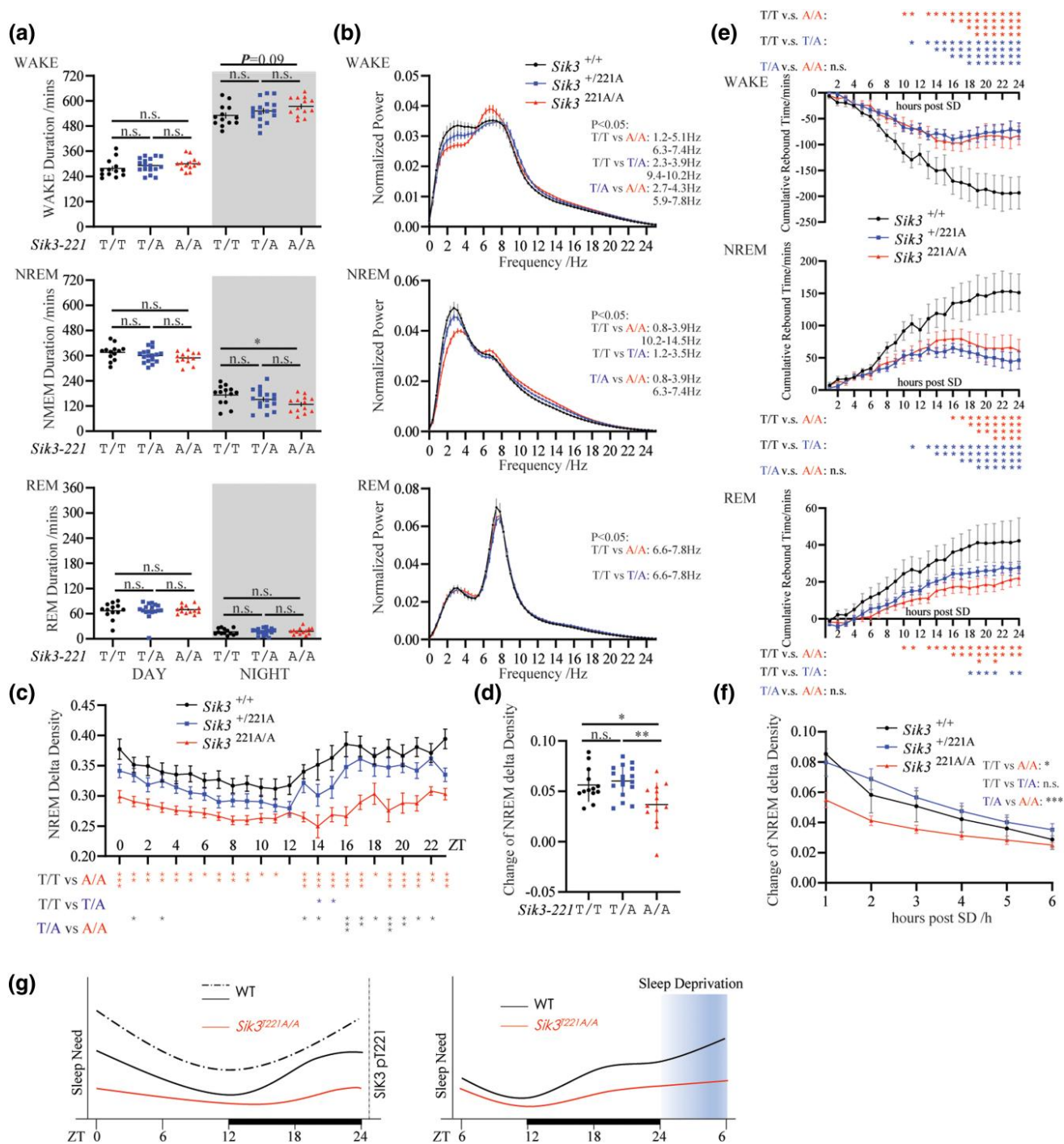


**Fig. 5.** T221 phosphorylation and sleep need in mice. a) The duration of WAKE, NREM and REM in *Sik3*<sup>+/+</sup> (n = 13), *Sik3*<sup>+/221A</sup> (n = 17), and *Sik3*<sup>221A/221A</sup> (n = 13). \*P < 0.05, Kruskal–Wallis test with Dunn’s posttest. Error bars represent SEM. b) EEG power spectrum of WAKE, NREM and REM states in *Sik3*<sup>+/+</sup> (n = 13), *Sik3*<sup>+/221A</sup> (n = 17), and *Sik3*<sup>221A/221A</sup> (n = 13). Two-way ANOVA with Tukey’s posttest, the P < 0.05 pairs was listed on the right. Error bars represent SEM. c) NREM  $\delta$ -power density of *Sik3*<sup>+/+</sup> (n = 13), *Sik3*<sup>+/221A</sup> (n = 17), and *Sik3*<sup>221A/221A</sup> (n = 13). Two-way ANOVA with Tukey’s posttest, statistical comparison among genotypes were listed below. \*P < 0.05, \*\*P < 0.01, \*\*\*P < 0.001. Error bars represent SEM. d)  $\delta$  power density increment from ZT9–11 to ZT19–24 of *Sik3*<sup>+/+</sup> (n = 13), *Sik3*<sup>+/221A</sup> (n = 17) and *Sik3*<sup>221A/221A</sup> (n = 13). Kruskal–Wallis test with Dunn’s posttest. \*P < 0.05, \*\*P < 0.01. Error bars represent SEM. e) Accumulated WAKE loss, and NREM, REM sleep gain of *Sik3*<sup>+/+</sup> (n = 6), *Sik3*<sup>+/221A</sup> (n = 10), and *Sik3*<sup>221A/221A</sup> (n = 8) after 6 hrs SD. Two-way ANOVA with Tukey’s posttest, \*P < 0.05, \*\*\*P < 0.001, \*\*\*\*P < 0.0001, Error bars represent SEM. f)  $\delta$  power density changes after SD at corresponding time points of *Sik3*<sup>+/+</sup> (n = 6), *Sik3*<sup>+/221A</sup> (n = 10), and *Sik3*<sup>221A/221A</sup> (n = 8) mice. For a given duration of time (T), changes (T) = post-SD density[T]–pre-SD density[T], Density[T] denotes the mean NREM  $\delta$  power density within T. Two-way ANOVA with Tukey’s posttest, \*P < 0.05, \*\*\*P < 0.001, Error bars represent SEM. g) A schematic illustration how SIK3-T221 phosphorylation indicates and controls sleep need in mice. The solid line is the sleep need and the dash line the phosphorylation level of SIK3-T221. The black line is WT and the red line T221A mutant.

(when mice had been awake for a night) was significantly less in T221A mutant mice than that in wt mice (Fig. 5d).  $\delta$  power EEG of T221A mutants were similar to wt mice during REM sleep (Fig. 5b). At all ZT points over 24 hrs, NREM delta power of

T221A mutants was significantly less than that in the wt mice (Fig. 5c), also consistent with a role for T221 in sleep need. These results indicate that T221 phosphorylation in SIK3 was required for sleep need.

We then analyzed rebound after SD in T221A mutant mice. After 6 hrs of SD from the onset of light phase, mice began to regain their lost NREM and REM sleep stages during the following 24 hrs (Fig. 5e). Both the NREM rebound and the REM rebound were significantly less in T221A mutant mice than those in wt mice (Fig. 5e).

$\delta$  density after SD was significantly lower in T221A mutant mice than that in wt mice (Supplementary Fig. 4c). Changes in  $\delta$  density after SD from corresponding baseline levels were also significantly less in T221A mutant mice than those in wt mice (Fig. 5f). Over the entire 24 hrs after SD, NREM  $\delta$  density was lower in T221A mice than that in the wt (Supplementary Fig. 4c).

It is notable that the sleep need phenotypes of T221A mutants (Fig. 5; Supplementary Fig. 4) were more significant than *Sik3*-*kof* mutants (Fig. 4; Supplementary Fig. 3), whereas the SIK3 protein level of *Sik3* Knockout first mice (Fig. 2, d and e) was lower than that in SIK3-T221A mutant mice (Fig. 2, f and g). In other words, the level of SIK3 protein without T221 phosphorylation in SIK3-T221A mutant mice was higher than SIK3 protein in *Sik3* Knockout first mice but sleep phenotype of SIK3-T221 mice was stronger than the sleep phenotype of SIK3 knockout first mice, suggesting the importance of T221 phosphorylation.

These results show that T221 phosphorylation in SIK3 was required for sleep need, for changes of sleep need during a regular daily sleep/wake cycle and for changes of sleep need after SD. T221 is also required for sleep rebound after SD.

## Discussion

Our results have demonstrated that phosphorylation of T221 in SIK3 is both an indicator and controller of sleep need in mammalian animals. Because other candidates, such as other kinases (SIK1 and SIK2) or the S551 in SIK3, do not satisfy the criteria, SIK3-T221 is the first indicator and controller of sleep need, at this point.

Our model is summarized in Fig. 5g: the left panel shows a natural daily sleep/wake cycle. The two solid lines represent sleep need (wt in black and SIK3-T221 mutants in red) and the dotted line represents T221 phosphorylation in the wt mice. Sleep need and SIK3-T221 phosphorylation increase during the WAKE stages (or the dark phase for mice); sleep need and SIK3-T221 phosphorylation decrease during the SLEEP stages (or the light phase for mice). When T221 is mutated to A221, the increase of sleep need during the WAKE stages is significantly reduced. The right panel shows effects of SD. Sleep need and T221 phosphorylation are increased by SD. T221A mutation reduces sleep need increase caused by SD and reduces sleep rebound after SD.

This model is supported by multiple pieces of evidence presented in this paper. We have found that sleep need and sleep need accumulation in mice were decreased by a LOF mutation of SIK3 (*Sik3*-*kof*) (Fig. 4), demonstrating a physiological requirement of SIK3 in sleep need. Phosphorylation of T221 in SIK3 monitored sleep need in mice: T221 phosphorylation increased with the loss of sleep during a natural daily sleep/wake cycle and T221 phosphorylation decreased with sleep (Fig. 3a). Artificial SD increased T221 phosphorylation (Fig. 3f). Functionally, sleep need and need accumulation rate were reduced in T221A mutant mice (Fig. 5, c and d) and sleep rebound after SD was also reduced in T221A mutant mice (Fig. 5e), both supporting that T221 phosphorylation controls sleep need.

Our results that T221 phosphorylation enhances both the catalytic activity of SIK3 and the stability of SIK3 provide mechanistic basis to understand the function of T221 phosphorylation. It will

be very interesting to study enzymes and mechanisms regulating T221 phosphorylation.

Our results with *Sik3*-*kof* mutants support that SIK3 is necessary for sleep need. Both sleep need measured by the  $\delta$  power of EEG and sleep rebound after SD were decreased in *Sik3*-*kof* mice. By contrast, while GOF mutations in SIK1 and SIK2 increased sleep need (Honda et al. 2018; Park et al. 2020), we report findings here that LOF mutations of SIK1 (Supplementary Fig. 1) or SIK2 (Supplementary Fig. 2) did not change sleep need, thus there is no evidence supporting that either SIK1 or SIK2 is physiologically necessary for sleep need in mice.

On the other hand, while the S551 site in SIK3 functionally important for sleep need (Funato et al. 2016; Honda et al. 2018), but MS measurement found no change in S551 phosphorylation after SD. This result did not support S551 as an indicator of sleep need.

S551 was phosphorylated by PKA and its phosphorylation inhibited SIK3 activity. Previous findings of increased sleep need with higher SIK3 activity in *Sleepy* and S551A mutants (Funato et al. 2016; Honda et al. 2018; Park et al. 2020) can be re-interpreted to support the idea that SIK3 activity indicates and controls sleep need, complementing our results from *Sik3*-*kof* and SIK3-T221A mutants. It will be interesting to examine in *Sleepy* and S551A mutant mice whether sleep rebound after SD is increased with higher SIK3 activity in these mutant mice, which would further support a role for SIK3 activity in controlling sleep need. It will also be interesting to investigate whether T221 phosphorylation is increased in *Sleepy* and S551A mutant mice. A finding of increased T221 phosphorylation in *Sleepy* and S551A mutants will support that T221 is the key to monitor and control sleep need. If T221 phosphorylation is not increased in *Sleepy* and S551A mutants, it will suggest that S551 may regulate SIK3 activity in other manners or that it regulates other proteins downstream of SIK3 such as 14-3-3 to control sleep need (Sonntag et al. 2018).

The sleep phenotypes of *+/-Sik3*-*kof* mice were sometimes similar to those of *+/+* mice and other times similar to those of *Sik3*-*kof*/*Sik3*-*kof* mice (Fig. 4), paralleling the fact that the dosages SIK3 protein (Fig. 2d) in *+/-Sik3*-*kof* mice were in-between those of *+/+* mice and *Sik3*-*kof*/*Sik3*-*kof* mice. Similarly, sleep phenotypes of *+/-T221A* mice were sometimes similar to those of *+/+* mice and other times similar to those of T221A/T221A mice (Fig. 5), with the dosage of SIK3 protein in *+/-T221A* mice also in-between those of *+/+* mice and T221A/T221A mice (Fig. 2f).

SIKs were found more than two decades ago (Feldman et al. 2000; Z. Wang et al. 1999; Xia et al. 2000) and belong to adenosine monophosphate-activated protein kinase (AMPK)-related kinases. Unlike AMPK, SIKs do not monitor cellular energy levels (Sakamoto et al. 2018). SIKs play multiple physiological roles (Darling and Cohen 2021) such as bone development (Sasagawa et al. 2012; Wein et al. 2016), circadian rhythms (Fujii et al. 2017; Hayasaka et al. 2017; Jagannath et al. 2013), metabolism (Patel et al. 2014; Sakamoto et al. 2018) and sleep (Funato et al. 2016; Grubbs et al. 2020; Honda et al. 2018; Park et al. 2020), and pathological roles (Darling and Cohen 2021; Wein et al. 2018) such as inflammation (Clark et al. 2012; Darling et al. 2017; Katoh et al. 2006) and cancer (Hollstein et al. 2019; Murray et al. 2019; Patra et al. 2018; Sun et al. 2020; Tarumoto et al. 2020; Zhou et al. 2017). It is curious whether other members of the AMPK related kinases play roles in sleep need or sleep.

Within their kinase domains, T182 in SIK1, T175 in SIK2 and T221 in SIK3 are equivalent to T172 in the catalytic  $\alpha$  subunit of AMPK (Clark et al. 2012; Darling et al. 2017; Katoh et al. 2006; Lizcano et al. 2004). T172 is important for AMPK $\alpha$  function, but it is not known whether T172 phosphorylation in AMPK $\alpha$  is

regulated by sleep or sleep need. It will be interesting to investigate the potential regulation of AMPK $\alpha$  T172 phosphorylation by sleep, the functional significance of AMPK $\alpha$  T172 phosphorylation in sleep and the potential roles of sleep-regulated AMPK $\alpha$  T172 phosphorylation in metabolic regulation.

Sleep is a crucial physiological process conserved in animals (Keene and Duboue 2018). There are two SIKs in *Drosophila* (Okamoto et al. 2004) and one in the worm *C. elegans* (Grubbs et al. 2020; Lanjuin and Sengupta 2002). It will be interesting to investigate their roles in sleep need, if reliable measure for sleep need can be established.

Molecular understanding of sleep regulation has heavily relied on the genetic approach, especially in the mouse and *Drosophila* by others and us over the last two decades (Shi et al. 2019, 2021; Zhang et al. 2018). A breakthrough in understanding chemical changes associated with or responsible for regulating sleep need should stimulate further mechanistic research into sleep need and homeostatic regulation of sleep.

It has not escaped our notice that the chemical indication we have discovered immediately suggests a novel approach to study endogenous mechanisms and exogenous means that regulate sleep.

## Data availability

Strains and plasmids are available upon request. The authors affirm that all data necessary for confirming the conclusions of the article are present within the article, figures, and tables.

Supplemental material available at GENETICS online.

## Acknowledgments

We are grateful to Dr. Juan Huang at CIBR for generating SIK mutant mice, Dr. Enxing Zhou for earlier participation in the project, Dr. Lei Zhang at CIBR instrument core for help with customizing experimental devices for EEG recording, the National Center for Protein Sciences at Peking University for access to instrumentation.

## Funding

This research was supported by Shenzhen Bay, Peking-Tsinghua Center for Life Sciences, Chinese Institute for Brain Research, and the Chinese Academy of Medical Sciences (2019RU003).

## Conflict of interest statement

The authors declare no conflicts of interests.

## Literature cited

- Allada R, White NE, So WV, Hall JC, Rosbash M. 1998. A mutant *Drosophila* homolog of mammalian clock disrupts circadian rhythms and transcription of period and timeless. *Cell*. 93(5):791–804. doi:10.1016/S0092-8674(00)81440-3.
- Barger Z, Frye CG, Liu D, Dan Y, Bouchard KE. 2019. Robust, automated sleep scoring by a compact neural network with distributional shift correction. *PLoS One*. 14(12):e0224642. doi:10.1371/journal.pone.0224642.
- Berggreen C, Henriksson E, Jones HA, Morrice N, Göransson O. 2012. Camp-elevation mediated by beta-adrenergic stimulation inhibits salt-inducible kinase (SIK) 3 activity in adipocytes. *Cell Signal*. 24(9):1863–1871. doi:10.1016/j.cellsig.2012.05.001.
- Borbély AA. 1982. A two process model of sleep regulation. *Hum Neurobiol*. 1(3):195–204.
- Borbély AA, Daan S, Wirz-Justice A, Deboer T. 2016. The two-process model of sleep regulation: a reappraisal. *J Sleep Res*. 25(2):131–143. doi:10.1111/jsr.12371.
- Cirelli C. 2009. The genetic and molecular regulation of sleep: from fruit flies to humans. *Nat Rev Neurosci*. 10(8):549–560. doi:10.1038/nrn2683.
- Clark K, MacKenzie KF, Petkevicius K, Kristariyanto Y, Zhang J, Choi HG, Peggie M, Plater L, Pedrioli PG, McIver E et al. 2012. Phosphorylation of CRTC3 by the salt-inducible kinases controls the interconversion of classically activated and regulatory macrophages. *Proc Natl Acad Sci U S A*. 109(42):16986–16991. doi:10.1073/pnas.1215450109.
- Crocker A, Sehgal A. 2010. Genetic analysis of sleep. *Genes Dev*. 24(12):1220–1235. doi:10.1101/gad.1913110.
- Daan S, Beersma DG, Borbely AA. 1984. Timing of human sleep: recovery process gated by a circadian pacemaker. *Am J Physiol*. 246(2 Pt 2):R161–R183. doi:10.1152/ajpregu.1984.246.2.R161.
- Dai X, Zhou E, Yang W, Mao R, Zhang W, Rao Y. 2021. Molecular resolution of a behavioral paradox: sleep and arousal are regulated by distinct acetylcholine receptors in different neuronal types in *Drosophila*. *Sleep*. 44(7):zsab017. doi:10.1093/sleep/zsab017.
- Dai X, Zhou E, Yang W, Zhang X, Zhang W, Rao Y. 2019. D-serine made by serine racemase in *Drosophila* intestine plays a physiological role in sleep. *Nat Commun*. 10(1):1986. doi:10.1038/s41467-019-09544-9.
- Darling NJ, Cohen P. 2021. Nuts and bolts of the salt-inducible kinases (SIKs). *Biochem J*. 478(7):1377–1397. doi:10.1042/BCJ20200502.
- Darling NJ, Toth R, Arthur JS, Clark K. 2017. Inhibition of SIK2 and SIK3 during differentiation enhances the anti-inflammatory phenotype of macrophages. *Biochem J*. 474(4):521–537. doi:10.1042/BCJ20160646.
- Deng B, Li Q, Liu X, Cao Y, Li B, Qian Y, Xu R, Mao R, Zhou E, Zhang W et al. 2019. Chemoconnectomics: mapping chemical transmission in *Drosophila*. *Neuron*. 101(5):876–893.e4. doi:10.1016/j.neuron.2019.01.045.
- Dijk DJ, Beersma DG, Daan S. 1987. EEG power density during nap sleep: reflection of an hourglass measuring the duration of prior wakefulness. *J Biol Rhythms*. 2(3):207–219. doi:10.1177/074873048700200304.
- Donlea JM, Ramanan N, Shaw PJ. 2009. Use-dependent plasticity in clock neurons regulates sleep need in *Drosophila*. *Science*. 324(5923):105–108. doi:10.1126/science.1166657.
- Donlea JM, Thimman MS, Suzuki Y, Gottschalk L, Shaw PJ. 2011. Inducing sleep by remote control facilitates memory consolidation in *Drosophila*. *Science*. 332(6037):1571–1576. doi:10.1126/science.1202249.
- Feldman JD, Vician L, Crispino M, Hoe W, Baudry M, Herschman HR. 2000. The salt-inducible kinase, SIK, is induced by depolarization in brain. *J Neurochem*. 74(6):2227–2238. doi:10.1046/j.1471-4159.2000.0742227.x.
- Franken P, Chollet D, Tafti M. 2001. The homeostatic regulation of sleep need is under genetic control. *J Neurosci*. 21(8):2610–2621. doi:10.1523/JNEUROSCI.21-08-02610.2001.
- Fujii S, Emery P, Amrein H. 2017. SIK3-HDAC4 signaling regulates *Drosophila* circadian male sex drive rhythm via modulating the DN1 clock neurons. *Proc Natl Acad Sci U S A*. 114(32):E6669–E6677. doi:10.1073/pnas.1620483114.

- Funato H, Miyoshi C, Fujiyama T, Kanda T, Sato M, Wang Z, Ma J, Nakane S, Tomita J, Ikkyu A *et al.* 2016. Forward-genetics analysis of sleep in randomly mutagenized mice. *Nature*. 539(7629): 378–383. doi:10.1038/nature20142.
- Grubbs JJ, Lopes LE, van der Linden AM, Raizen DM. 2020. A salt-induced kinase is required for the metabolic regulation of sleep. *PLoS Biol.* 18(4):e3000220. doi:10.1371/journal.pbio.3000220.
- Hardin PE, Hall JC, Rosbash M. 1990. Feedback of the *Drosophila* period gene product on circadian cycling of its messenger RNA levels. *Nature*. 343(6258):536–540. doi:10.1038/343536a0.
- Hayasaka N, Hirano A, Miyoshi Y, Tokuda IT, Yoshitane H, Matsuda J, Fukada Y. 2017. Salt-inducible kinase 3 regulates the mammalian circadian clock by destabilizing PER2 protein. *Elife*. 6:e24779. doi:10.7554/eLife.24779.
- Hendricks JC, Finn SM, Panckeri KA, Chavkin J, Williams JA, Sehgal A, Pack AI. 2000. Rest in *Drosophila* is a sleep-like state. *Neuron*. 25(1):129–138. doi:10.1016/S0896-6273(00)80877-6.
- Henriksson E, Jones HA, Patel K, Peggie M, Morrice N, Sakamoto K, Göransson O. 2012. The AMPK-related kinase SIK2 is regulated by camp via phosphorylation at SER358 in adipocytes. *Biochem J.* 444(3):503–514. doi:10.1042/BJ20111932.
- Hollstein PE, Eichner LJ, Brun SN, Kamireddy A, Svensson RU, Vera LI, Ross DS, Rymoff TJ, Hutchins A, Galvez HM *et al.* 2019. The AMPK-related kinases SIK1 and SIK3 mediate key tumor-suppressive effects of LKB1 in NSCLC. *Cancer Discov.* 9(11): 1606–1627. doi:10.1158/2159-8290.CD-18-1261.
- Honda T, Fujiyama T, Miyoshi C, Ikkyu A, Hotta-Hirashima N, Kanno S, Mizuno S, Sugiyama F, Takahashi S, Funato H *et al.* 2018. A single phosphorylation site of SIK3 regulates daily sleep amounts and sleep need in mice. *Proc Natl Acad Sci U S A.* 115(41):10458–10463. doi:10.1073/pnas.1810823115.
- Jagannath A, Butler R, Godinho SIH, Couch Y, Brown LA, Vasudevan SR, Flanagan KC, Anthony D, Churchill GC, Wood MJA *et al.* 2013. The CRTCL1-SIK1 pathway regulates entrainment of the circadian clock. *Cell.* 154(5):1100–1111. doi:10.1016/j.cell.2013.08.004.
- Katoh Y, Takemori H, Lin XZ, Tamura M, Muraoka M, Satoh T, Tsuchiya Y, Min L, Doi J, Miyauchi A *et al.* 2006. Silencing the constitutive active transcription factor CREB by the LKB1-SIK signaling cascade. *FEBS J.* 273(12):2730–2748. doi:10.1111/j.1742-4658.2006.05291.x.
- Keene AC, Duboue ER. 2018. The origins and evolution of sleep. *J Exp Biol.* 221(11):jeb159533. doi:10.1242/jeb.159533.
- King DP, Zhao Y, Sangoram AM, Wilsbacher LD, Tanaka M, Antoch MP, Steeves TD, Vitaterna MH, Kornhauser JM, Lowrey PL *et al.* 1997. Positional cloning of the mouse circadian clock gene. *Cell.* 89(4):641–653. doi:10.1016/S0092-8674(00)80245-7.
- Konopka RJ, Benzer S. 1971. Clock mutants of *Drosophila melanogaster*. *Proc Natl Acad Sci U S A.* 68(9):2112–2116. doi:10.1073/pnas.68.9.2112.
- Lanjuin A, Sengupta P. 2002. Regulation of chemosensory receptor expression and sensory signaling by the KIN-29 Ser/Thr kinase. *Neuron*. 33(3):369–381. doi:10.1016/S0896-6273(02)00572-X.
- Liu S, Liu Q, Tabuchi M, Wu MN. 2016. Sleep drive is encoded by neural plastic changes in a dedicated circuit. *Cell.* 165(6):1347–1360. doi:10.1016/j.cell.2016.04.013.
- Lizcano JM, Göransson O, Toth R, Deak M, Morrice NA, Boudeau J, Hawley SA, Udd L, Makela TP, Hardie DG *et al.* 2004. LKB1 is a master kinase that activates 13 kinases of the AMPK subfamily, including MARK/PAR-1. *EMBO J.* 23(4):833–843. doi:10.1038/sj.emboj.7600110.
- MacKenzie KF, Clark K, Naqvi S, McGuire VA, Noehren G, Kristariyanto Y, van den Bosch M, Mudaliar M, McCarthy PC, Pattison MJ, *et al.* 2013. PGE(2) induces macrophage IL-10 production and a regulatory-like phenotype via a protein kinase A-SIK-CRTC3 pathway. *J Immunol.* 190(2):565–577. doi:10.4049/jimmunol.1202462.
- Murray CW, Brady JJ, Tsai MK, Li C, Winters IP, Tang R, Andrejka L, Ma RK, Kunder CA, Chu P *et al.* 2019. An LKB1-SIK axis suppresses lung tumor growth and controls differentiation. *Cancer Discov.* 9(11):1590–1605. doi:10.1158/2159-8290.CD-18-1237.
- Okamoto M, Takemori H, Katoh Y. 2004. Salt-inducible kinase in steroidogenesis and adipogenesis. *Trends Endocrinol Metab.* 15(1): 21–26. doi:10.1016/j.tem.2003.11.002.
- Park M, Miyoshi C, Fujiyama T, Kakizaki M, Ikkyu A, Honda T, Choi J, Asano F, Mizuno S, Takahashi S *et al.* 2020. Loss of the conserved PKA sites of SIK1 and SIK2 increases sleep need. *Sci Rep.* 10(1): 8676. doi:10.1038/s41598-020-65647-0.
- Patel K, Foretz M, Marion A, Campbell DG, Gourlay R, Boudaba N, Tournier E, Titchenell P, Peggie M, Deak M *et al.* 2014. The LKB1-salt-inducible kinase pathway functions as a key gluconeogenic suppressor in the liver. *Nat Commun.* 5(1):4535. doi:10.1038/ncomms5535.
- Patra KC, Kato Y, Mizukami Y, Widholz S, Boukhali M, Revenco I, Grossman EA, Ji F, Sadreyev RI, Liss AS *et al.* 2018. Mutant GNAS drives pancreatic tumorigenesis by inducing PKA-mediated SIK suppression and reprogramming lipid metabolism. *Nat Cell Biol.* 20(7):811–822. doi:10.1038/s41556-018-0122-3.
- Qian Y, Cao Y, Deng B, Yang G, Li J, Xu R, Zhang D, Huang J, Rao Y. 2017. Sleep homeostasis regulated by 5HT2b receptor in a small subset of neurons in the dorsal fan-shaped body of *Drosophila*. *Elife*. 6:e26519. doi:10.7554/eLife.26519.
- Renn SC, Park JH, Rosbash M, Hall JC, Taghert PH. 1999. A PDF neuropeptide gene mutation and ablation of PDF neurons each cause severe abnormalities of behavioral circadian rhythms in *Drosophila*. *Cell.* 99(7):791–802. doi:10.1016/S0092-8674(00)81676-1.
- Sakamoto K, Bultot L, Göransson O. 2018. The salt-inducible kinases: emerging metabolic regulators. *Trends Endocrinol Metab.* 29(12): 827–840. doi:10.1016/j.tem.2018.09.007.
- Sasagawa S, Takemori H, Uebi T, Ikegami D, Hiramatsu K, Ikegawa S, Yoshikawa H, Tsumaki N. 2012. SIK3 is essential for chondrocyte hypertrophy during skeletal development in mice. *Development.* 139(6):1153–1163. doi:10.1242/dev.072652.
- Sehgal A, Price JL, Man B, Young MW. 1994. Loss of circadian behavioral rhythms and per RNA oscillations in the *Drosophila* mutant timeless. *Science.* 263(5153):1603–1606. doi:10.1126/science.8128246.
- Shaw PJ, Cirelli C, Greenspan RJ, Tononi G. 2000. Correlates of sleep and waking in *Drosophila melanogaster*. *Science.* 287(5459): 1834–1837. doi:10.1126/science.287.5459.1834.
- Shi G, Xing L, Wu D, Bhattacharyya BJ, Jones CR, McMahon T, Chong SYC, Chen JA, Coppola G, Geschwind D *et al.* 2019. A rare mutation of beta(1)-adrenergic receptor affects sleep/wake behaviors. *Neuron.* 103(6):1044–1055.e7. doi:10.1016/j.neuron.2019.07.026.
- Shi G, Yin C, Fan Z, Xing L, Mostovoy Y, Kwok PY, Ashbrook LH, Krystal AD, Ptáček LJ, Fu YH. 2021. Mutations in metabotropic glutamate receptor 1 contribute to natural short sleep trait. *Curr Biol.* 31(1):13–24.e4. doi:10.1016/j.cub.2020.09.071.
- Sonntag T, Vaughan JM, Montminy M. 2018. 14-3-3 Proteins mediate inhibitory effects of camp on salt-inducible kinases (SIKS). *FEBS J.* 285(3):467–480. doi:10.1111/febs.14351.
- Sun Z, Jiang Q, Li J, Guo J. 2020. The potent roles of salt-inducible kinases (SIKS) in metabolic homeostasis and tumorigenesis. *Signal Transduct Target Ther.* 5(1):150. doi:10.1038/s41392-020-00265-w.
- Suzuki A, Sinton CM, Greene RW, Yanagisawa M. 2013. Behavioral and biochemical dissociation of arousal and homeostatic sleep need

- influenced by prior wakeful experience in mice. *Proc Natl Acad Sci U S A*. 110(25):10288–10293. doi:[10.1073/pnas.1308295110](https://doi.org/10.1073/pnas.1308295110).
- Takemori H, Katoh Y, Horike N, Doi J, Okamoto M. 2002. Acth-induced nucleocytoplasmic translocation of salt-inducible kinase. Implication in the protein kinase a-activated gene transcription in mouse adrenocortical tumor cells. *J Biol Chem*. 277(44):42334–42343. doi:[10.1074/jbc.M204602200](https://doi.org/10.1074/jbc.M204602200).
- Tarumoto Y, Lin S, Wang J, Milazzo JP, Xu Y, Lu B, Yang Z, Wei Y, Polyanskaya S, Wunderlich M et al. 2020. Salt-inducible kinase inhibition suppresses acute myeloid leukemia progression in vivo. *Blood*. 135(1):56–70. doi:[10.1182/blood.2019001576](https://doi.org/10.1182/blood.2019001576).
- Tobler I, Borbély AA. 1986. Sleep EEG in the rat as a function of prior waking. *Electroencephalogr Clin Neurophysiol*. 64(1):74–76. doi:[10.1016/0013-4694\(86\)90044-1](https://doi.org/10.1016/0013-4694(86)90044-1).
- Toh KL, Jones CR, He Y, Eide EJ, Hinz WA, Virshup DM, Ptáček LJ, Fu YH. 2001. An hper2 phosphorylation site mutation in familial advanced sleep phase syndrome. *Science*. 291(5506):1040–1043. doi:[10.1126/science.1057499](https://doi.org/10.1126/science.1057499).
- Wang B, Moya N, Niessen S, Hoover H, Mihaylova MM, Shaw RJ, Yates JR, Fischer WH, Thomas JB, Montminy M. 2011. A hormone-dependent module regulating energy balance. *Cell*. 145(4):596–606. doi:[10.1016/j.cell.2011.04.013](https://doi.org/10.1016/j.cell.2011.04.013).
- Wang Z, Takemori H, Halder SK, Nonaka Y, Okamoto M. 1999. Cloning of a novel kinase (SIK) of the SNF1/ampk family from high salt diet-treated rat adrenal. *FEBS Lett*. 453(1–2):135–139. doi:[10.1016/S0014-5793\(99\)00708-5](https://doi.org/10.1016/S0014-5793(99)00708-5).
- Wein MN, Foretz M, Fisher DE, Xavier RJ, Kronenberg HM. 2018. Salt-inducible kinases: physiology, regulation by camp, and therapeutic potential. *Trends Endocrinol Metab*. 29(10):723–735. doi:[10.1016/j.tem.2018.08.004](https://doi.org/10.1016/j.tem.2018.08.004).
- Wein MN, Liang Y, Goransson O, Sundberg TB, Wang J, Williams EA, O'Meara MJ, Govea N, Beqo B, Nishimori S et al. 2016. SIKs control osteocyte responses to parathyroid hormone. *Nat Commun*. 7(1):13176. doi:[10.1038/ncomms13176](https://doi.org/10.1038/ncomms13176).
- Werth E, Dijk DJ, Achermann P, Borbély AA. 1996. Dynamics of the sleep EEG after an early evening nap: experimental data and simulations. *Am J Physiol*. 271(3 Pt 2):R501–R510. doi:[10.1152/ajpregu.1996.271.3.R501](https://doi.org/10.1152/ajpregu.1996.271.3.R501).
- Xia Y, Zhang Z, Kruse U, Vogt PK, Li J. 2000. The new serine-threonine kinase, Qik, is a target of the Qin oncogene. *Biochem Biophys Res Commun*. 276(2):564–570. doi:[10.1006/bbrc.2000.3508](https://doi.org/10.1006/bbrc.2000.3508).
- Xu Y, Padiath QS, Shapiro RE, Jones CR, Wu SC, Saigoh N, Saigoh K, Ptáček LJ, Fu YH. 2005. Functional consequences of a CKIdelta mutation causing familial advanced sleep phase syndrome. *Nature*. 434(7033):640–644. doi:[10.1038/nature03453](https://doi.org/10.1038/nature03453).
- Xu Y, Toh KL, Jones CR, Shin JY, Fu YH, Ptáček LJ. 2007. Modeling of a human circadian mutation yields insights into clock regulation by PER2. *Cell*. 128(1):59–70. doi:[10.1016/j.cell.2006.11.043](https://doi.org/10.1016/j.cell.2006.11.043).
- Zhang X, Yan H, Luo Y, Huang Z, Rao Y. 2018. Thermoregulation-independent regulation of sleep by serotonin revealed in mice defective in serotonin synthesis. *Mol Pharmacol*. 93(6):657–664. doi:[10.1124/mol.117.111229](https://doi.org/10.1124/mol.117.111229).
- Zhou J, Alfraidi A, Zhang S, Santiago-O'Farrill JM, Yerramreddy Reddy VK, Alsaadi A, Ahmed AA, Yang H, Liu J, Mao W et al. 2017. A novel compound ARN-3236 inhibits salt-inducible kinase 2 and sensitizes ovarian cancer cell lines and xenografts to paclitaxel. *Clin Cancer Res*. 23(8):1945–1954. doi:[10.1158/1078-0432.CCR-16-1562](https://doi.org/10.1158/1078-0432.CCR-16-1562).

Editor: T. Caspary